ELSEVIER

Chemical Engineering Science 62 (2007) 957–968

Chemical Engineering Science

www.elsevier.com/locate/ces

PEM fuel cell current regulation by fuel feed control

Claire H. Woo, J.B. Benziger*

Department of Chemical Engineering, Princeton University, Princeton, NJ 08544, USA

Received 15 August 2006; received in revised form 23 October 2006; accepted 24 October 2006
Available online 7 November 2006

Abstract

We demonstrate that the power output from a PEM fuel cell can be directly regulated by limiting the hydrogen feed to the fuel cell. Regulation is accomplished by varying the internal resistance of the membrane–electrode assembly in a self-draining fuel cell with the effluents connected to water reservoirs. The fuel cell functionally operates as a dead-end design where no gas flows out of the cell and water is permitted to flow in and out of the gas flow channel. The variable water level in the flow channel regulates the internal resistance of the fuel cell. The hydrogen and oxygen (or air) feeds are set directly to stoichiometrically match the current, which then control the water level internal to the fuel cell. Standard PID feedback control of the reactant feeds has been incorporated to speed up the system response to changes in load. With dry feeds of hydrogen and oxygen, 100% hydrogen utilization is achieved with 130% stoichiometric feed on the oxygen. When air was substituted for oxygen, 100% hydrogen utilization was achieved with stoichiometric air feed. Current regulation is limited by the size of the fuel cell (which sets a minimum internal impedance), and the dynamic range of the mass flow controllers. This type of regulation could be beneficial for small fuel cell systems where recycling unreacted hydrogen may be impractical.

Keywords: PEM fuel cells; Fuel cell control; Fuel utilization; Efficiency; Impedance matching

1. Introduction

Fuel cells and batteries are electrochemical power supplies. A chemical potential difference provides a driving force to push an ionic current through an electrolyte and an electronic current through an external load. In simple circuit terms, the chemical potential difference produces a voltage (battery voltage V_b) that drives the current (i_L) through the internal electrolyte resistance (R_i) and an external load resistance (R_L) (Wilkinson and Vanderleeden, 2003). The useful power delivered to the load (P_L) is the current through the circuit multiplied by the voltage drop across the load. The schematic of a simple hydrogen/oxygen fuel cell with a polymer membrane electrolyte is shown in Fig. 1, along with a simplified Thevenin equivalent circuit. This model is simpler than most fuel cell models presented in the literature (Xue et al., 2004; Hsuen, 2004; Pathapati et al., 2004; Wang, 2004; Weber and Newman, 2004), but is sufficient for analysis of the feedback control.

The fuel cell current, as given by Eq. (1), depends on the load impedance connected across the fuel cell. For simplicity we assume that the fuel cell operation is limited to the ohmic regime. To account for kinetic barriers at the electrode surfaces the battery voltage is assumed to be a constant effective potential which is generally ~ 300 mV less than the thermodynamic potential ($V_b \sim 0.9$ V).

$$i_L = \frac{V_b}{(R_i + R_L)}, \tag{1a}$$

$$P_L = i_L^2 R_L = \frac{V_b^2 R_L}{(R_i + R_L)^2}. \tag{1b}$$

In order to control the power delivered to the external load either the battery voltage, the effective load resistance or the internal resistance must be varied.

1.1. Controlling power output from a fuel cell

A fuel cell is part of an electric circuit where the typical objective is to control the power delivered to the load impedance.

* Corresponding author. Tel.: +1 609 258 5416.
E-mail address: benziger@princeton.edu (J.B. Benziger).

0009-2509/$ - see front matter © 2006 Elsevier Ltd. All rights reserved.
doi:10.1016/j.ces.2006.10.027

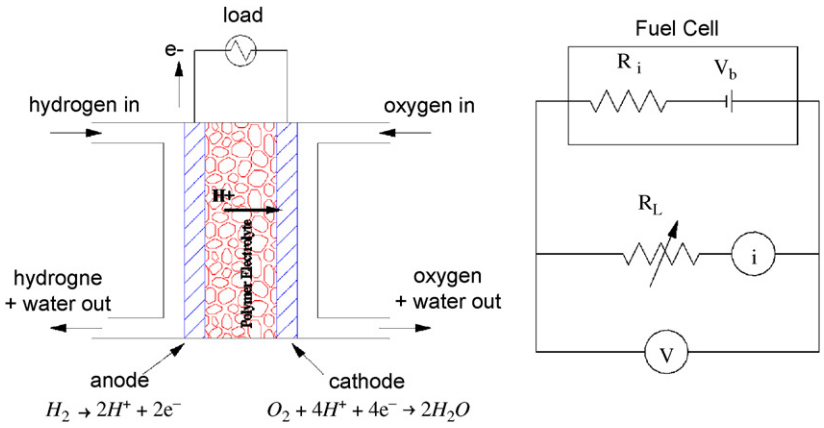

Fig. 1. Schematic of a PEM fuel cell and the simplified equivalent circuit.

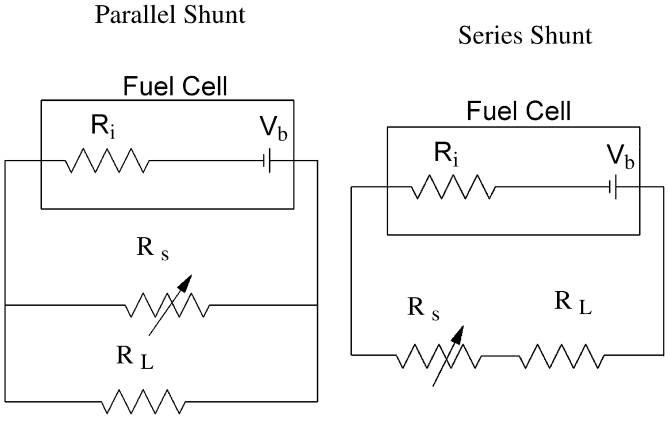

Fig. 2. A shunt resistor can be added in series or in parallel to the load to control current.

The simplest and most common means of controlling the power to the load is to vary the effective load resistance seen by the battery or fuel cell by adding a shunt resistance; this is sometimes referred to as linear control (Larminie and Lowry, 2003). The shunt resistor, with resistance R_s, can be placed in series or in parallel to the load. The choice of which configuration is employed is based on the importance of controllability and fuel efficiency. Excess power is dissipated in the shunt resistor; thus fuel efficiency is sacrificed to permit simple control. The series and parallel shunt circuits are shown in Fig. 2. The power and efficiency for the two arrangements are shown in Fig. 3 as functions of the ratio of the shunt resistance to the load impedance (R_s/R_L) for a ratio of load impedance to internal resistance of 1 ($R_L/R_i = 1$). The process gain (i.e., the change in power output with change in shunt resistance) is greatest when the shunt resistance is less than the load resistance (i.e., $R_s/R_L < 1$). Large process gain is beneficial for process control. The series shunt allows for higher fuel efficiency at conditions where controllability is best.

The energy efficiency shown in Fig. 3 is based on the useful power delivered through the load relative to the fuel conversion. A battery is a closed system that can convert all its reactants to electrical energy. However, fuel cells generally require excess reactants to remove the product water in the effluent streams. Typically, as the total external impedance is varied, the feed to a fuel cell is maintained at a pre-defined stoichiometry or fuel utilization. Most fuel cells are operated under excess hydrogen feed (Barbir, 2005; Larminie and Dicks, 2003). Pukrushpan et al. (2004), Suh and Stefanopoulou (2005) and Sun and Kolmanovsky (2005) assert that excess hydrogen and oxygen feed is necessary to avoid operational problems such as stagnant water vapor, catalyst degradation and accumulation of impurities. High velocity gas also serves the purpose of removing excess water produced by the redox reaction at the cathode. Thus, mass flow controllers are often used to keep the stoichiometric ratio for hydrogen at about 2 ($\lambda_{H_2} = H_2$ fed/ H_2 reacted $= 2$) as the external impedance is changed, limiting the single-pass fuel efficiency to 50% (Wilkinson and Vanderleeden, 2003; Larminie and Dicks, 2003; Yu et al., 2005). To achieve reasonable fuel efficiency it is necessary to utilize the unreacted fuel; in a small system producing electricity the fuel would be recycled, which would involve a recompression stage prior to mixing it with fresh feed.

An alternative method of changing the power output from a fuel cell is changing the partial pressure of the reactants, thus altering the battery voltage. Lorenz et al. (1997) and Mufford and Strasky (1998) obtained patents for controlling power by variable air inflow to a fuel cell, but we found no reports of successful implementation of this latter scheme.

A final possibility to control the power output from a fuel cell or battery would be to control the cell's internal resistance. This might be accomplished by varying temperature in a solid oxide fuel cell, or varying the membrane water content in a polymer electrolyte membrane (PEM) fuel cell (Chen et al., 2005). Altering the internal resistance is equivalent to adding a series shunt resistance to the circuit. However, we have found no reports in the literature successfully controlling the internal resistance of the electrode/electrolyte assembly.

1.2. Fuel utilization efficiency

The chemical to electrical energy conversion is less efficient for fuel cells than for batteries. Batteries are closed systems.

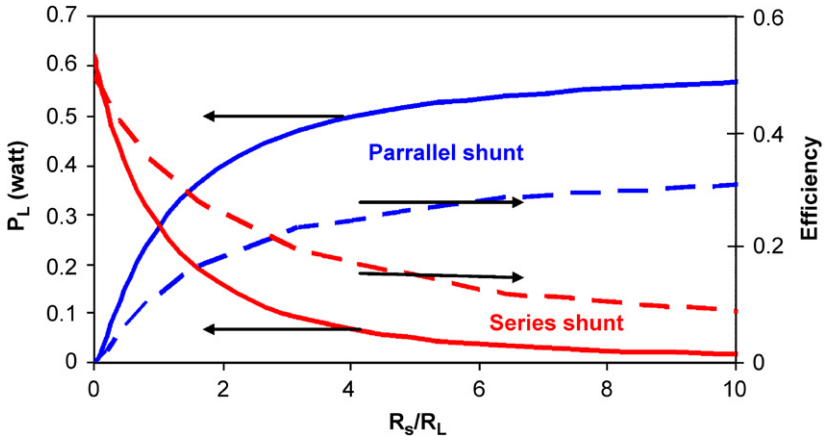

Fig. 3. Power and efficiency for two different shunt resistor strategies ($R_i = R_L = 0.4\,\Omega$). The power is the useful power dissipated in the load resistor and the efficiency is the ratio of useful power to the total power dissipated.

Reaction only occurs when an external load is connected across the battery, permitting current to flow. The chemical reaction can be turned on and off by switching the load on and off, and there is no loss of chemical energy from unreacted fuel leaving the battery. (There is a long-term self-discharging of batteries which we will neglect here.) Fuel cells are open systems where the reactants are continuously fed to the cell and products (water in the case of a hydrogen fuel cell) are continuously removed. Excess reactants are fed to the fuel cell to maintain the voltage, and the excess fuel is either discarded or recycled. Processing the excess fuel reduces the fuel efficiency. There is a minimum excess fuel requirement for flow through fuel cells; experience with serpentine flow channels found that when the stoichiometric excess of the reactant flow approaches zero, mass transfer limitations result in a large internal voltage drop (Lee et al., 2006; Zawodzinski et al., 2000; Quan et al., 2005).

Control of a fuel cell system would be greatly simplified if one could manipulate the power output simply by controlling the feed to the fuel cell, as is done with internal combustion engines (Lumley, 1999; Stone, 1999). Here, we introduce a new conceptual approach to regulating the power output by varying the effective internal resistance of a PEM fuel cell through liquid water management. The effective size, and hence the effective resistance, of the fuel cell can be controlled by balancing the reactant feed and the reaction rate (current) with no net outflow. We report experimental results showing that the current output from a PEM fuel cell can be regulated directly by limiting the flow of hydrogen and oxygen to the fuel cell. From here on, we will call this control method "current control by fuel regulation". We also determine experimentally the limits for the practical application of this type of regulation.

Fuel cell process control is dominated by the dynamics of reaction and transport. Power conditioning electronics such as voltage converters and load governors are fast and can be used for impedance matching (Caux et al., 2005; Correa et al., 2004; El-Sharkh et al., 2004). However, the electronics control disregards the more intricate changes that occur in the fuel cell, including changes in temperature, relative humidity and membrane conductivity, all of which affect output at a longer response time. Lauzze and Chmielewski (2006) developed a model to simulate PEM fuel cell response to feedback power control by varying the load resistance, cell temperature, relative humidity and air feed. The complex dynamics of a fuel cell are evident in the complex coupling of control parameters. We will look explicitly at the fuel cell response to changes in reactant flow rate and external load impedance which are the system parameters that are manipulated in PEM fuel cell systems. We have not included any power conversion electronics control at this stage of testing.

2. Experimental

Experiments were conducted with custom built stirred tank reactor (STR) fuel cells based on the design of Hogarth and Benziger (2006) and Benziger et al. (2004). The contact area between the gas phase and the membrane–electrode assembly (MEA) was 1.9 cm^2. The anode and cathode were diamond shaped gas plenums machined from graphite with pillars to improve pressure uniformity on the MEA. The fuel cell was placed in an insulated temperature-controlled environment. Tests reported here were done with Nafion/carbon cloth MEAs fabricated in our lab. Nafion 115 membranes (Ion Power Inc., DE, USA) were cleaned using a standard procedure (sequential boiling for 1 h each in 3 wt% peroxide, DI water, 1 M sulfuric acid and DI water). The Nafion was sandwiched between A6 ELAT-type electrodes (E-tek division of Denora, NJ, USA) which contained 0.5 mg/cm^2 of Pt on carbon. The carbon paper was coated with 0.6 mg/cm^2 of 5 wt% Nafion solution to improve contact at the three phase interface (Raistrick, 1989). MEAs were pressed at 140 °C for 90 s at 40 MPa pressure before being placed into the cells. Four bolts on the cell were each tightened to 3 N m of torque.

The current and voltage across the load resistor were measured and logged by a computer. A 10-turn 0–20 Ω potentiometer was manually adjusted for the desired load, which was

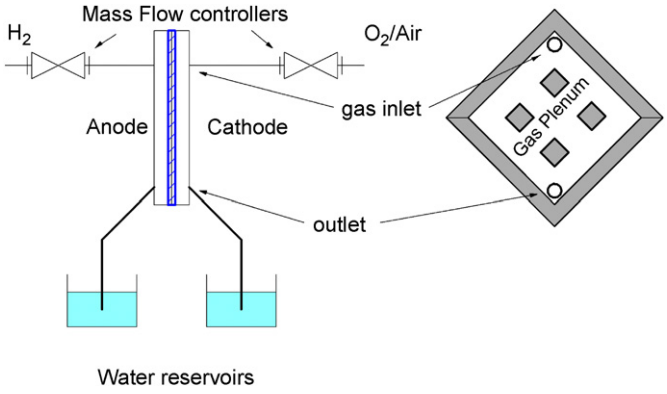

Fig. 4. Schematic of the self-draining PEM fuel cell configuration.

usually kept constant at values between 0.5 and 3 Ω. The voltage across the load resistor was read directly by a DAQ board. The current through the load resistor was passed through a 0.1 Ω sensing resistor and the differential voltage across the sensing resistor was read by the DAQ board in order to calculate the current.

Hydrogen and oxygen were supplied from commercial cylinders (Airco) through mass flow controllers (Aalborg Instruments); the mass flow rate and voltage setpoint for the flow rate were connected to the DAQ board. Compressed air was substituted for the oxygen for experiments with air. The unique feature of the fuel cell is that it is self-draining. Any liquid water formed falls by gravity to the outlets of the gas plenums. The effluents drained into water reservoirs that prohibited any back diffusion of gases to either electrode as shown in Fig. 4. The water baths collected the liquid water product for both the anode and cathode in graduated cylinders.

Eq. (2) is the overall mole balance of hydrogen in the fuel cell. At steady state and 100% hydrogen utilization, no hydrogen exits the cell, so Eq. (2) simplifies to Eq. (3), which is the governing equation for the tests reported here. The output current of a single STR fuel cell connected to a fixed load resistance was controlled by varying the hydrogen feed flow rate Q_A^{in}. Similar equations can be derived for the oxygen mole balance. A feedback control loop was set up in LabTech Notebook program for controlling the output current of the fuel cell by adjusting the feed gas flow rates.

$$\frac{V_A}{RT}\frac{\mathrm{d}P_{\mathrm{H_2}}^{\text{out}}}{\mathrm{d}t} = \left(\frac{Q_A^{\text{in}}P_{\mathrm{H_2}}^{\text{in}}}{RT} - \frac{Q_A^{\text{out}}P_{\mathrm{H_2}}^{\text{out}}}{RT}\right) - \frac{i}{2\mathrm{F}}, \tag{2}$$

$$\frac{i}{2\mathrm{F}} = \frac{Q_A^{\text{in}}P_{\mathrm{H_2}}^{\text{in}}}{RT}. \tag{3}$$

3. Results

3.1. Current regulation by fuel feed control

We first illustrate direct control of the fuel cell current by fuel feed control. The self-draining STR fuel cell was configured to operate with dry feeds at 60 °C. A potentiometer was connected as the external load and set for a fixed resistance between 0.5 and 6 Ω. The H_2/O_2 flow rates were varied with constant stoichiometry from $\frac{1.5}{0.98}$ to $\frac{10}{6.5}$ mL/min. The steady-state current increased linearly with the hydrogen flow rate to a limiting current that depended on the load resistance (Fig. 5a). After the steady-state current reached its limiting value the steady-state current remained constant with any further increases in the hydrogen flow rate. At hydrogen flow rates below the limiting steady-state current no gas bubbles were seen exiting from the anode into the water reservoir. There was a stoichiometric excess of O_2 and gas bubbles were seen exiting from the cathode at all currents. When the hydrogen flow rate was increased above that corresponding to the limiting steady-state current, gas bubbles were observed exiting from the anode outlet into the water reservoir.

The limiting currents are summarized in Table 1 along with the hydrogen gas flow rate and the voltage drop across the load resistor. The fuel cell was operated at steady state for > 24 h at several temperature settings between 25 and 80 °C, load resistance from 0.5 to 3 Ω and gas flow rates from 1.5 mL/min to the limiting current flow. The water exiting from both the anode and cathode was collected. Table 1 shows excellent agreement in the balance between current and the water collected at the cathode at the limiting current conditions. When hydrogen utilization was 100% the water product was all collected at the cathode; the water volume in the anode reservoir remained constant. When the hydrogen flow was in excess of that corresponding to the limiting current, gas bubbles exited the anode and liquid water was collected from both the anode and cathode outlets.

Fig. 5 graphically summarizes the relationship between the fuel cell current, the hydrogen flow rate to the fuel cell and the voltage drop across the load resistor. The current scaled linearly with hydrogen flow rate as predicted by Eq. (3), up to the limiting current. The voltage drop across the load resistance (in the literature this is often referred to as the fuel cell voltage, Barbir, 2005; Larminie and Dicks, 2003) also varied linearly with current up to the limiting current. The voltage and current remained constant for increased hydrogen flow rate past the limiting conditions.

The power delivered by the fuel cell to a fixed load can be changed to any value up to the maximum for that load (specified in Table 1) simply by changing the hydrogen flow rate. The power increases quadratically with hydrogen flow rate since $P_L = i_L^2 R_L$.

Shown in Fig. 6 is the dynamic response of the fuel cell current to step changes in the hydrogen flow rate. For the fuel cell employed in these studies the open loop process time constant was ∼ 30 s.

The successful regulation of the current in a PEM fuel cell by hydrogen feed control initially surprised us. There are hypotheses for such a control scheme, but we could find no report in the literature where such a control scheme has been demonstrated. Indeed previous investigators were unable even to maintain a constant current with dead-end fuel cells (Pukrushpan et al., 2004; Lee et al., 2006; Zawodzinski et al., 2000; Quan et al.,

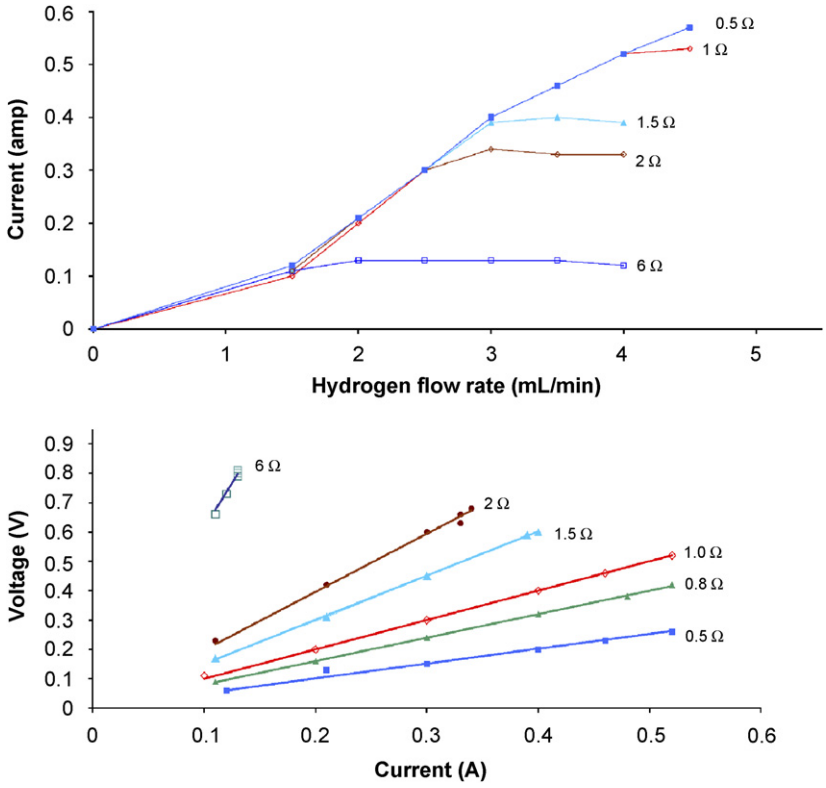

Fig. 5. Voltage–current and flow–current relations for the PEM fuel cell with current regulation by hydrogen feed control at the anode. The slope of the voltage current line is equal to the load resistance. The slope of the flow rate current line is given by Eq. (3) up to the limiting current.

Table 1
Limiting currents for 100% hydrogen utilization at 60 °C

Load resistance (Ω)	Max H_2 flow (sccm)	Max current (A)	ΔV_{max} (V)	Max power density (W/cm^2)	Water collected at cathode (mL/h)/(A)
0.5	6.0	0.810	0.405	0.173	NA
0.8	4.5	0.610	0.490	0.157	NA
1.0	4.0	0.530	0.530	0.148	0.38 (0.54)
1.5	3.5	0.410	0.610	0.132	0.27 (0.40)
2.0	2.5	0.345	0.690	0.125	0.21 (0.30)
6.0	1.0	0.110	0.810	0.048	NA

2005; Fabian et al.; Grujicic et al., 2004a,b; Wang et al., 2006). Our fuel cell design and operation is crucial in this type of direct control. Current regulation was achieved by a balance between the pressure in the cell and the water reservoir where the effluents discharged. Water could flow between the reservoir and the anode flow channel. Changing the water level in the anode flow channel altered the contact area between the gas and the electrode creating a variable internal resistance. We demonstrated this by attaching a pipette to the outlet of the anode as shown in Fig. 7. We observed that the liquid level in the pipette rose and fell in proportion to the hydrogen feed indicating water displacement from the anode flow channel. Table 2 summarizes the change in hydrostatic gas pressure in the anode as a function of the fuel cell current. The maximum hydrostatic pressure across the anode gas plenum is ~ 3.7 cm H_2O, in excellent agreement with the experimental results.

3.2. Feedback control of fuel feed for current regulation

The fuel cell response can be sped up by employing feedback control on the hydrogen flow rate based on the desired current (or power) setpoint. Fig. 8 is the response to a change in setpoint current when a PID controller was used to regulate the hydrogen flow rate. The load resistance was kept constant at 1 Ω, and the oxygen flow was set to a fixed rate of 5 mL/min while the hydrogen flow rate was manipulated to respond in response to the difference in current and the setpoint current. The PID controller was fine tuned from standard Ziegler–Nichols closed loop tuning to achieve a specified current between 100 and 500 mA (Seborg et al., 1989). The optimal control parameters are listed in Table 3. Fig. 8 shows the current and hydrogen flow rate as a function of time during two setpoint changes in the current at $t = 100$ and 200 s, respectively. The current

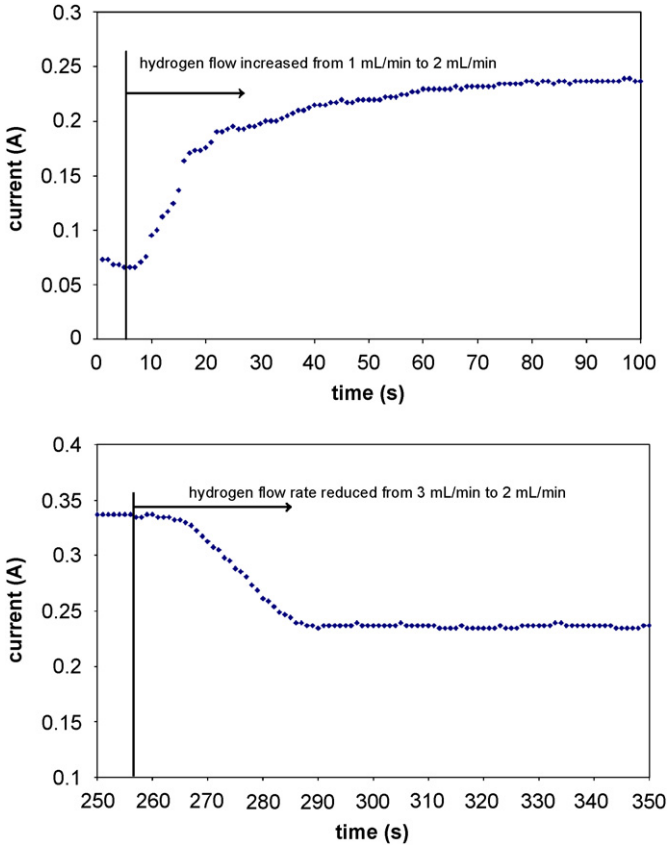

Fig. 6. Fuel cell current response to a step increase of the hydrogen flow rate at the anode from 1 (0.11 A) to 2 mL/min (0.24 A), and a step decrease from 3 (0.34 A) to 2 mL/min (0.24 A). The oxygen flow at the cathode was 5 mL/min in both cases.

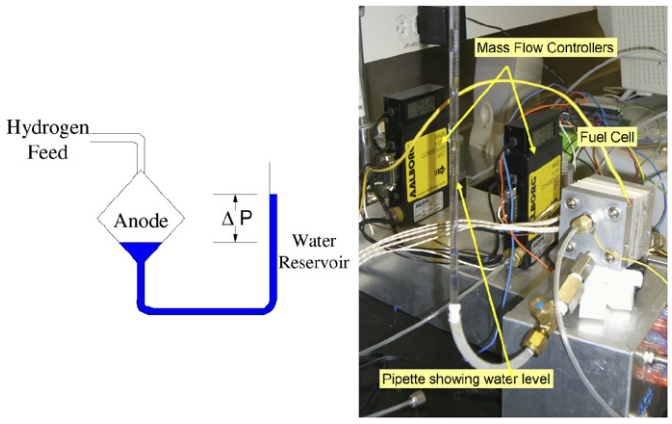

Fig. 7. Schematic of the fuel cell anode connected to an external water reservoir. The water flows in and out of the anode to maintain the total pressure in the gas flow channel equal to the external pressure. Water blocks active MEA area, which causes an increase in R_i and allows for dynamic control of the current by fuel feed. On the right is a photo of the actual experimental setup.

responds rapidly to changes in the setpoint as the hydrogen flow rate is adjusted by the PID controller, and steady-state is achieved in ~ 10 s with negligible overshoot. The steady state current shows little fluctuation or variation. The hydrogen flow rate shows non-negligible fluctuations which are probably due to pressure fluctuations at the anode.

Table 2
Anode hydrostatic pressure vs. current cell at 25 °C, with 1 Ω load

Current (A)	ΔP (cm H_2O)
0	0
0.05	1.0
0.1	1.2
0.15	1.4
0.2	1.7
0.3	2.5
0.4	3.5

Hydrogen utilization was 100% while the fuel cell current was under PID control. This was confirmed by two observations. First, there was no gas exiting the anode once steady state was reached. Second, the hydrogen feed exactly matched the current through the load resistor by the relationship shown in Eq. (3). However, with a 1 Ω load resistance the current could only be controlled between $\sim$ 50 and $\sim$ 530 mA. It was impossible to achieve currents greater than 530 mA with a 1 Ω load independent of the hydrogen flow rate. At current setpoints > 530 mA and $R_L = 1\,\Omega$ gas bubbles were observed at the anode outlet and the current maxed out at 530 mA.

There was also a minimum controllable current setpoint due to limitations in the mass flow controllers. The mass flow controllers could not accurately maintain a current setpoint below $\sim$ 50 mA (minimum flow rate controllable with the mass flow controller was ~ 0.5 mL/min).

After control by hydrogen flow regulation proved successful we tested control of the fuel cell current by limiting the oxygen flow. The fuel cell was fed with excess hydrogen (10 mL/min) and the oxygen flow was regulated to achieve a desired setpoint current. The PID controller constants were again determined for the fastest response with minimal overshoot; the optimal values are reported in Table 3. The fuel cell operated with 100% oxygen utilization at the cathode and excess hydrogen at the anode. The principal difference between regulating hydrogen or oxygen was that the system took much longer to stabilize under oxygen flow regulation, as illustrated in Fig. 9.

Next, both the anode and cathode feeds were regulated based on fixed stoichiometry. The difference between the current and the current setpoint was used to manipulate the hydrogen feed rate. The oxygen feed was slaved to be a constant stoichiometry relative to hydrogen. (This is a feedforward control on the oxygen feed and is analogous to a fixed fuel/air mixture to a combustion engine, where the stoichiometry is kept constant and the feed rate is increased or decreased to vary the power.) The optimal PID control parameters determined from the hydrogen flow regulation tests were employed. As shown in Fig. 10, the fuel cell current could not be controlled stably at 2:1 H_2:O_2 stoichiometry (i.e., 100% utilization of both H_2 and O_2). To test for stability, the fuel cell was run with different stoichiometric ratios of oxygen while the current was regulated by hydrogen feed control. The ratio of excess oxygen was increased little by little until stability was achieved. The results shown in Fig. 10

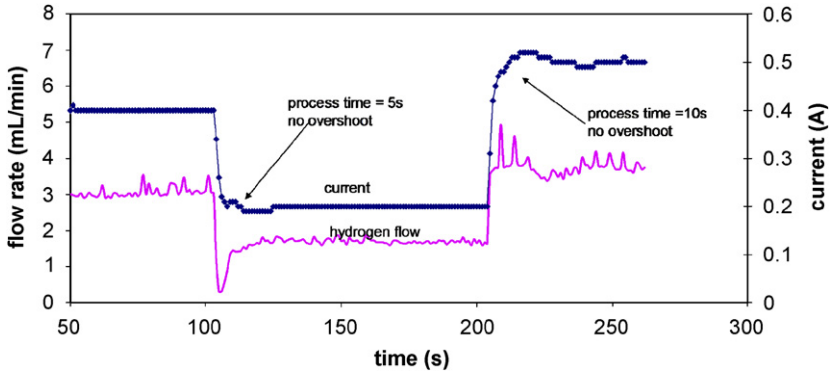

Fig. 8. Current regulation by hydrogen feed control at 60 °C with a load resistance. There is 100% utilization of hydrogen and nothing exits from the anode effluent.

Table 3
Optimized process controller constants

Hydrogen flow controlled, 0 < hydrogen flow < 4 mL/ min, oxygen flow = 5 mL/ min	Oxygen flow controlled, hydrogen flow = 10 mL/ min, 0 < oxygen Flow < 2 mL/ min
Gain = 1.3 $\tau_I = 0.4$ s $\tau_D = 0.07$ s	Gain = 6.0 $\tau_I = 3.0$ s $\tau_D = 1.2$ s

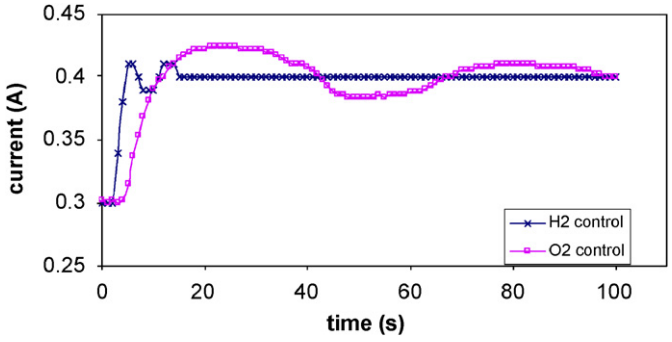

Fig. 9. Comparison of current regulation by H_2 or O_2 feed control at 60 °C. The current setpoint was changed from 0.3 to 0.4 A. Control by O_2 feed regulation took a much longer time to stabilize than control by H_2 feed regulation.

indicate that the fuel cell required a minimum oxygen flow of 30% excess to operate stably. At lower stoichiometric excess of oxygen the current eventually became unstable and oscillated.

The stability of the control and the water balances in the fuel cell were tested over periods of 24–72 h. Current regulation by hydrogen feed control operated stably over periods of 72 h. When operated with 100% hydrogen utilization and 30% oxygen excess, all the water formed in the fuel cell exited in the cathode effluent, as measured by graduated cylinders. The robustness of feedback control for current regulation was tested under different types of disturbances at three different operating temperatures. As shown in Fig. 11, the fuel cell recovered from changes in setpoint and load within seconds at temperatures between 25 and 80 °C. For a current setpoint change from 300 to 400 mA, the response time was under 10 s at all three temperatures. When H_2 flow was stopped for 5 s, the current was able to return to the setpoint value within 32–54 s. The fuel cell took longer to respond to disruptions in hydrogen flow at lower temperatures, possibly due to more liquid water present. After a reduction in load from 1 to 0.5 Ω the current was able to recover within 7–14 s.

The current regulation by hydrogen flow was repeated with air feed at the cathode (21% O_2). We hypothesized two possible reasons for the unstable control with < 30% excess oxygen. The first possibility is that liquid water formed at the cathode did not fully drain by gravity; some liquid remains at the gas plenum limiting the mass transfer of oxygen from the gas flow channel to the membrane/electrode interface. If this is true, feeding air to the cathode should reduce the problem since the higher gas flow with inert nitrogen would facilitate liquid water removal. An alternative possibility is that oxygen diffusion across the cathode gas diffusion layer is slower than hydrogen diffusion across the anode gas diffusion layer. Reducing the oxygen partial pressure at the cathode by replacing oxygen with air would cause the oxygen diffusion to be slower, in which case control would be worse with air than oxygen.

When the experiments were repeated with air feed, 100% H_2 and 100% O_2 utilization could be achieved. The current was maintained at a setpoint of 300 mA at 25 °C for > 4 h with 100% hydrogen utilization and a 2:5 feed ratio of hydrogen to air. Furthermore, as shown in Fig. 12, a setpoint change from 300 to 200 mA had a recovery time of 52 s whereas the reversed change from 200 to 300 mA had a recovery time of 19 s. This result indicates that water blockage of gas flow channels was responsible for the unstable current regulation. The presence of liquid water slowed the response time during oxygen starvation and necessitated excess oxygen for stable control.

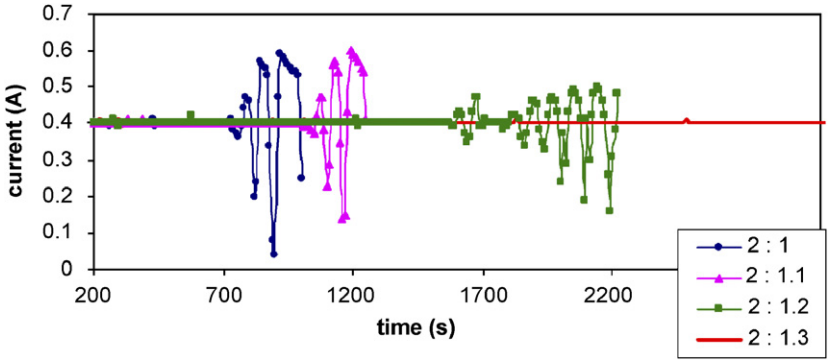

Fig. 10. Minimum ratio of H_2:O_2 feed to achieve stability under control by H_2 feed regulation. The legend indicates the ratio of H_2:O_2 feeds. Transient current at different ratios of H_2:O_2 flows showed that stability was maintained only when at least 30% excess O_2 was supplied.

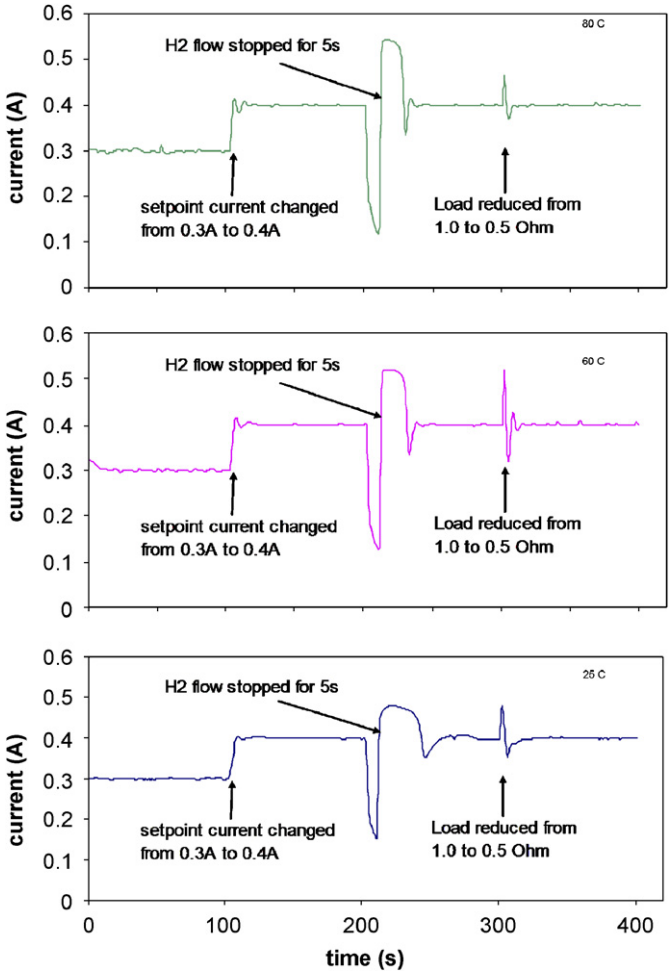

Fig. 11. Fuel cell response to three different disturbance tests—a setpoint change, H_2 flow disruption and a load change. The tests were performed at 25, 60, and 80 °C while the fuel cell was under H_2 starvation control with 30% excess O_2.

4. Discussion

Why have not previous attempts of current regulation by hydrogen feed control or oxygen feed control been successful? Previous efforts to regulate current based on reactant feed control attempted to control the battery voltage by changing the concentrations at the electrodes. The theoretical battery voltage, given by Eq. (4), depends logarithmically on the hydrogen partial pressure, so changing the partial pressure of hydrogen at the anode by an order of magnitude will only change the voltage by 4–5%.

$$V_b = \frac{\Delta G^0}{2F} + \frac{RT}{2F} \ln\left[P_{H_2}^{\text{anode}}\right] = 1.2 + 0.015 \ln\left[P_{H_2}^{\text{anode}}\right] \text{ V}. \quad (4)$$

The process gain for current regulation by controlling the hydrogen flow rate is given by

$$K_P = \frac{\partial i}{\partial Q_{H_2}} = 0.015 \frac{\partial \ln P_{H_2}}{\partial Q_{H_2}}. \quad (5)$$

To vary the current by an order of magnitude would require that partial pressure of hydrogen at the anode to be changed by five orders of magnitude. Water formation further constrains the operating pressure. The total pressure in the anode flow channel equals the sum of the hydrogen partial pressure and water partial pressure, $P_{\text{total}} = P_w + P_{H_2}$. The hydrogen pressure will vary between the total pressure and the total pressure less the saturation vapor pressure of water at the fuel cell temperature, $P_{\text{total}} > P_{H_2} \geqslant P_{\text{total}} - P_w^0(T)$. The only way to have the hydrogen partial pressure change substantially is for the total pressure at the electrode to change, which is not very practical.

The "self-draining" fuel cell design we employed combines advantages of both flow-through designs and dead-end designs. The gas flow at the anode is dead-ended, but the liquid flow at the anode is flow-through. To accomplish this it is necessary to have precise balance over the pressure at the anode. The pressure differences are cm of water (1 cm $H_2O \approx 10^{-3}$ bar).

We are not the first to employ dead-end PEM fuel cells. PEM fuel cells are commercially available that operate dead-ended (e.g. The Fuel Cell Store http://www.fuelcellstore.com and H Tech Inc., http://www.thehydrogencompany.com), but they employ serpentine flow channels that do not permit self-draining by gravity (Lee et al., 2006; McLean, 2003). These systems require periodic purging to remove the liquid water from the flow channels.

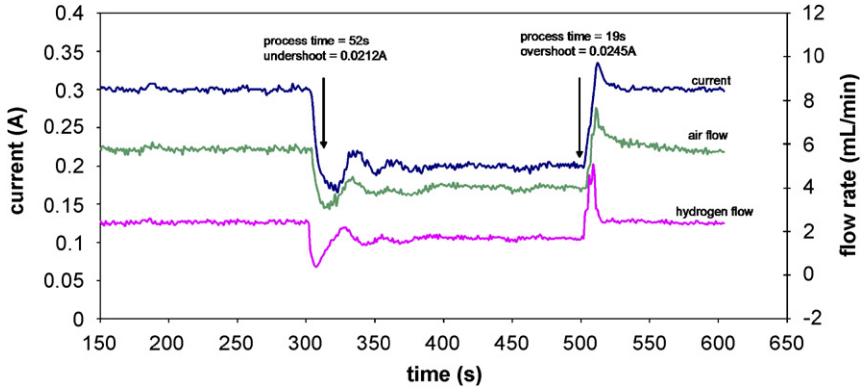

Fig. 12. Fuel cell response to setpoint changes in current during control by combined H_2 and O_2 starvation under air feed at 25 °C and with a constant load of 1 Ω. Setpoint current was changed from 300 to 200 at $t = 300$ s and from 200 to 300 mA at $t = 400$ s.

Most fuel cells use a flow-through design with stoichiometric excesses of both hydrogen and oxygen. The total flow is slaved to the current and the current is controlled with load governor. Typically the flow of reactants is about twice stoichiometric. But problems are encountered at low currents when the gas velocity in the flow channels is low and liquid water slugs in the flow channels create current and voltage fluctuations.

The unique features of our fuel cell design are: (1) it is self-draining (the water drains to the bottom of the flow channels under gravity) and (2) the effluents are connected to water reservoirs which maintain a constant pressure in the flow channels. The pressure in the water reservoirs fixes the total pressure inside the flow channels of the fuel cell. If the pressure inside the flow channel is higher than that in the water reservoir, gas flows out of the channel to reduce the pressure and bubbles into the water. On the other hand, if the pressure is lower in the flow channel, water will flow into the flow channel compressing the gas until the internal and external pressures are equalized. In other words, the water level in the flow channels adjusts to equalize the hydrostatic pressures in the reservoir and the gas in the flow channel. As the water flows in and out of the flow channel it alters the effective area of the MEA, thus changing the internal resistance of the fuel cell.

At 100% utilization, the gas volume at the anode is determined by a balance between the hydrogen feed rate and the removal of hydrogen to form water. Combining Eqs. (1b) and (3), we obtain Eq. (6) which relates the hydrogen flow rate to the internal resistance of the fuel cell:

$$\frac{P_{H_2}^{in} Q_{H_2}}{RT} = \frac{i}{2F} = \frac{V_b}{2F} \frac{1}{R_i + R_L}. \tag{6}$$

We operated the fuel cell with the water reservoir open to the atmosphere, so that the total pressure in the flow channels was always 1 bar. Since liquid water is present in the flow channel, the water vapor pressure is the saturation pressure at the fuel cell temperature. Hence, the hydrogen partial pressure at the anode must be constant, which in turn means that the battery voltage V_b is constant. As the water level changes in the fuel cell, the available MEA area for transporting protons changes, meaning that the internal resistance also changes. The internal resistance of the MEA scales inversely with its area, where $R_i = \frac{\rho_m}{A_m}$. Water present in the gas flow channels blocks active MEA area, effectively increasing the internal resistance of the fuel cell. Eq. (6) can be rearranged to Eq. (7) to determine the active MEA area as a function of hydrogen flow rate for the required current:

$$A_m = \frac{\rho_m}{(V_b/2F)RT/Q_{H_2} P_{H_2}^{in} - R_L}. \tag{7}$$

Changing the hydrogen flow rate causes the water level in the anode to adjust to a height where the supply and removal of hydrogen are in balance.

We demonstrated this dynamic equilibrium by attaching a 0.5 mL pipette to the anode outlet; the results are summarized in Table 2. When the fuel cell was operated under hydrogen feed control, the water level in the pipette connected to the anode would rise and fall as the setpoint current was changed, confirming that the MEA area was changing.

The dynamic pressure adjustment between the anode flow channel and the water reservoir sets limits on the range of current regulation. The highest current corresponds to a flow rate where the liquid water is completely pushed out of the anode flow channel and the internal resistance is a minimum ($R_{i,\min}$). In the current fuel cell design the membrane resistance is $\sim 0.75\,\Omega\,cm^2$ ($R_{i,\min} = 0.4\,\Omega$). The internal resistance of the fuel cell was obtained from the slope of the *IV* curve (polarization curve). Assuming an effective battery voltage of 0.8 V the maximum current for a 1 Ω load resistance is 570 mA. It is not possible to get a higher current by increasing the hydrogen flow rate.

The minimum current that can be regulated is determined by the lowest flow rate the mass flow controller can accurately maintain, $Q_{H_2}^{min}$. The minimum flow rate sets limits on the maximum load impedance, $R_{L,\max}$, for which the current can be regulated by hydrogen flow control:

$$R_{L,\max} < \frac{RT}{Q_{H_2}^{min} P_{H_2}^{in}} \frac{V_b}{2F} < R_{i,\min}, \tag{8}$$

where $R_{i,\min}$ is the minimum internal resistance when the anode is free of liquid water. The mass flow controller is stable to

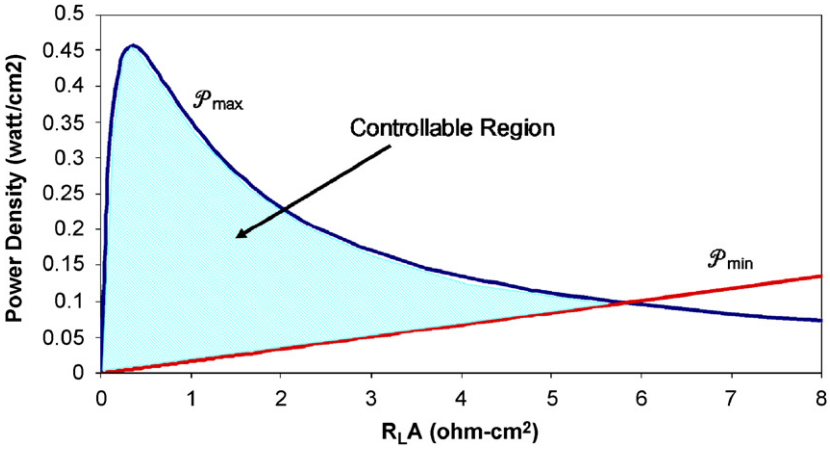

Fig. 13. Controllable region of power control by fuel feed control in a PEM fuel cell. The minimum power is set by the limit on mass flow control to the fuel cell, the maximum power is set by the minimum internal resistance of the fuel cell.

$\sim$ 1% full scale, which is 0.5 mL/min in our system. The minimum flow rate that can be controlled is $\sim$1–2% full scale, or $\sim$ 1 mL/ min. The accuracy of controlling a low flow is evident in Fig. 5a where there is a slightly different slope of current vs. hydrogen flow rate at the lowest flow rates. The maximum controllable load for our fuel cell is predicted to be $\sim 6\,\Omega$. In our tests, we found that the current became uncontrollable for load resistances $> 4\,\Omega$.

The regime for power regulation from the PEM fuel cell by hydrogen flow control can be generalized in terms of power density (watts per unit area) as a function of load resistance normalized by the fuel cell size. The maximum power delivered to the load is limited by the load resistance, membrane resistivity and battery voltage as given by Eq. (9). The minimum controllable power depends on the minimum controllable flow rate and the load resistance as given by

$$P_{\max} = \frac{V_b^2 (R_L A_m)}{(\rho_m + R_L A_m)^2}, \tag{9}$$

$$P_{\min} = \left(2\mathbb{F}\frac{Q_{\mathrm{H_2,min}} P_{\mathrm{H_2}}}{A_m R T}\right)^2 (R_L A_m). \tag{10}$$

These equations define a region where regulation of power by feed control is realizable (see Fig. 13). The dynamic range of power regulation is the vertical distance between the maximum and minimum lines. The dynamic range of power regulation is greatest where the power curve goes through its maximum, which is where the load resistance matches the internal resistance of the fuel cell. The dynamic range of power regulation decreases when the load resistance exceeds the internal resistance. Power regulation becomes impossible for loads greater than the maximum resistance defined by Eq. (8). Control is most effective when the load impedance matches the internal resistance of the fuel cell! This is also the condition when the power delivered by the fuel cell to the load is maximized (Benziger et al., 2006).

The key to feed control of power regulation is the self-draining fuel cell design. This permits a small pressure differential of $\sim$ 100 Pa (1 cm of water) to move liquid in and out of the fuel cell gas space and alter the effective volume. We have successfully implemented this control scheme with a three-cell stack for current densities $< 200\,\mathrm{mA/cm^2}$ (Woo, 2006). The water level rises and falls in all cells simultaneously to respond to the current control. At higher current densities the power fluctuated. We believe the common manifold for liquid water drainage was improperly sized to handle the liquid water flow from all three cells at higher current densities.

There are two important restrictions to current or power regulation by fuel feed control. First is that the hydrogen must be free of any significant impurities. Our experiments used electronic grade H_2 (99.999%, < 1 ppm CO). High-purity gases are necessary to operate dead-ended for extended periods of time. We demonstrated continuous operation for > 72 h without needing to purge the anode of accumulated impurities. The second restriction to current regulation by fuel feed control is that liquid water should be present. The operating pressure of the fuel cell and water reservoir should be at least twice the vapor pressure of water at the fuel cell temperature. Operating at 1 bar total pressure limits the maximum temperature to 80 °C.

There have been reports that starvation of the reactants to the fuel cell accelerates electrode degradation (Meyers and Darling, 2006). We operated our fuel cell over a period of $\sim$ 1000 h with multiple start-up and shut-down cycles with no significant degradation in the power output. Our system does not starve the electrodes in the way most other systems operate during start-up and shut-down. Most fuel cells have effluents that are open to the atmosphere, so when they are shut down air can back up into the anode. The membrane can dry out, and during start-up the hydrogen–oxygen combustion reaction will occur at the anode producing excess heat. In the fuel cell design we presented here, water from the reservoirs fills the anode and cathode plenums at shut-down so the membrane is always protected. At start-up gas displaces the water. This system does have a down-side when exposed to freezing environments since the formation of ice will block the gas flow.

The effective utilization of fuel and power can be improved by power conditioning employing voltage converters and by recycling of unreacted fuel (Schumacher et al., 2004; Tekin et al., 2006; Zenith and Skogestad, 2006). These additions to the overall fuel cell system increase its overall complexity. Implementation of fuel recycling is only viable for larger scale fuel cell systems—the economic penalty associated with systems smaller than 1 kW will be prohibitive. For small systems batteries have always had an efficiency advantage over fuel cells because they have 100% fuel utilization. Current regulation with fuel feed control provides a simple solution to meet a variable power demand for a fixed load with 100% fuel utilization. We envision that such a solution can make fuel cells competitive with batteries for small power systems. We also point out that our fuel cell employed dry feeds, eliminating any need for humidifiers at either the anode or the cathode. System simplification by using dry feeds and controlling power output by fuel supply are two key elements needed to reduce the balance of plant and make small fuel cells practical.

5. Conclusions

We have demonstrated that the PEM fuel cell current may be regulated directly by hydrogen feed control with 100% fuel utilization. This system can deliver variable power to a fixed load without any need for fuel recycling. Current regulation was achieved by connecting the outlets of a self-draining fuel cell to water reservoirs. A dynamic balance of liquid water in the anode flow channel and the reservoir varies the internal resistance of the fuel cell, thus regulating the current. A hydrogen/air PEM fuel cell was operated with dry feeds at exact stoichiometry with complete utilization of the hydrogen and the oxygen. When feeding pure oxygen to the cathode, a minimum oxygen flow rate of 130% stoichiometric was required for stable regulation of the current. Limits on power output were derived based on the load resistance, the size of the fuel cell and the minimum controllable feed flow. Current (or power) regulation by fuel feed control not only improves fuel efficiency but also simplifies the control system and eliminates the need for additional infrastructure for recycling excess fuel.

Notation

A_m	active area of membrane–electrode assembly, cm^2
F	Faraday's constant (96469 C/mol)
ΔG^0	free energy of fuel cell reaction
i	current, amp
K_P	process gain
P_{H_2}	partial pressure of hydrogen, bar
P_w	water vapor pressure, bar
P_{total}	total gas pressure, bar
P	power delivered to the load impedance, W
Q_{H_2}	hydrogen flow rate, mL/min
R	gas constant
R_i	internal resistance of membrane–electrode assembly, Ω
R_L	load resistance, Ω
R_s	shunt resistance, Ω
T	temperature
V_b	battery voltage of fuel cell

Greek letter

ρ_m	membrane resistivity

Acknowledgments

This work was supported by the NSF CTS-0354279. C. Woo was supported as an REU student by the NSF Grant DMR 0455186. We thank Ioannis Kevrekidis for his helpful suggestions during this work.

References

Barbir, F., 2005. PEM Fuel Cells: Theory and Practice. Elsevier, Academic Press, Burlington, MA.

Benziger, J., Chia, E., Karnas, E., Moxley, J., Teuscher, C., Kevrekidis, I.G., 2004. The stirred tank reactor polymer electrolyte membrane fuel cell. A.I.Ch.E. Journal 50 (8), 1889–1900.

Benziger, J.B., Satterfield, M.B., Hogarth, W.H.J., Nehlsen, J.P., Kevrekidis, I.G., 2006. The power performance curve for engineering analysis of fuel cells. Journal of Power Sources 155 (2), 272–285.

Caux, S., Lachaize, J., Fadel, M., Shott, P., Nicod, L., 2005. Modelling and control of a fuel cell system and storage elements in transport applications. Journal of Process Control 15 (4), 481–491.

Chen, F.L., Chu, H.S., Soong, C.Y., Yan, W.M., 2005. Effective schemes to control the dynamic behavior of the water transport in the membrane of PEM fuel cell. Journal of Power Sources 140 (2), 243–249.

Correa, J.M., Farret, F.A., Canha, L.N., Simoes, M.G., 2004. An electrochemical-based fuel-cell model suitable for electrical engineering automation approach. IEEE Transactions on Industrial Electronics 51 (5), 1103–1112.

El-Sharkh, M.Y., Rahman, A., Alam, M.S., Sakla, A.A., Byrne, P.C., Thomas, T., 2004. Analysis of active and reactive power control of a stand-alone PEM fuel cell power plant. IEEE Transactions on Power Systems 19 (4), 2022–2028.

Fabian, T., O'Hayre, R., Litster, S., Prinz, F.B., Santiago, J.G., Water management at the cathode of a planar airbreathing fuel cell with an electroosmotic pump.⟨http://ecsmeet2.peerxpress.org/ms_files/ecsmeet2/2006/05/25/00041654/00/41654_0_art_file_0_1148596230.pdf⟩.

Grujicic, M., Chittajallu, K.M., Law, E.H., Pukrushpan, J.T., 2004a. Model-based control strategies in the dynamic interaction of air supply and fuel cell. Proceedings of the Institution of Mechanical Engineers Part A 218 (A7), 487–499.

Grujicic, M., Chittajallu, K.M., Pukrushpan, J.T., 2004b. Control of the transient behaviour of polymer electrolyte membrane fuel cell systems. Proceedings of the Institution of Mechanical Engineers Part D 218 (D11), 1239–1250.

Hogarth, W.H.J, Benziger, J.B., 2006. Operation of polymer electrolyte membrane fuel cells with dry feeds: design and operating strategies. Journal of Power Sources 159, 968–978.

Hsuen, H.-K., 2004. Performance equations of polymer electrolyte fuel cells. Journal of Power Sources 126, 46–57.

Larminie, J., Dicks, A., 2003. Fuel Cell Systems Explained, second ed. Wiley, New York.

Larminie, J., Lowry, J., 2003. Electric Vehicle Technology Explained. Wiley, Chicester, UK.

Lauzze, K.C., Chmielewski, D.J., 2006. Power control of a polymer electrolyte membrane fuel Cell. Industrial and Engineering Chemistry Research 45 (13), 4661–4670.

Lee, Y., Kim, Y., Kim, J.C., Chung, J.T., 2006. Performance characteristics of a polymer electrolyte fuel cell with the anodic supply mode. ⟨http://ecsmeet2.peerxpress.org/ms_files/ecsmeet2/2006/05/26/00041765/00/41765_0_art_file_1_1148616666.pdf⟩.

Lorenz, H., Noreikat, K.-E., Klaiber, T., et al., 1997. Daimler-Benz Aktiengesellschaft, assignee. Method and device for vehicle fuel cell dynamic power control. US Patent No. 5646852, July.

Lumley, J.L., 1999. Engines: an Introduction. Cambridge University Press, New York.

McLean, G.F., 2003. Angstrom power (CA), assignee. Apparatus of high power density fuel cell layer with micro for connecting to an external load. US Patent No. 6864010, January 22.

Meyers, J.P., Darling, R.M., 2006. Model of carbon corrosion in PEM fuel cells. Journal of the Electrochemical Society 153 (8), A1432–A1442.

Mufford, W.E., Strasky, D.G., 1998. DBB fuel cell engines GmbH, assignee. Power control system for a fuel cell powered vehicle. US Patent No. 5771476, June.

Pathapati, P.R., Xue, X., Tang, J., 2004. A new dynamic model for predicting transient phenomena in a PEM fuel cell system. Renewable Energy 30 (1), 1–22.

Pukrushpan, J.T., Stefanopoulou, A.G., Peng, H., 2004. Control of fuel cell breathing. IEEE Control Systems Magazine 24 (2), 30–46.

Quan, P., Zhou, B., Sobiesiak, A., Liu, Z.S., 2005. Water behavior in serpentine micro-channel for proton exchange membrane fuel cell cathode. Journal of Power Sources 152 (1), 131–145.

Raistrick, I.D., 1989. US Department of energy, assignee. Electrode assembly for use in a solid polymer electrolyte fuel cell. US Patent No. 4876115, October 24.

Schumacher, J.O., Gemmar, P., Denne, M., Zedda, M., Stueber, M., 2004. Control of miniature proton exchange membrane fuel cells based on fuzzy logic. Journal of Power Sources 129 (2), 143–151.

Seborg, D., Edgar, T., Mellichamp, D., 1989. Process Dynamics and Control. Wiley, New York.

Stone, R., 1999. Introduction to Internal Combustion Engines. Society of Automotive Engineers, Warrendale, PA.

Suh, K.W., Stefanopoulou, A.G., 2005. Coordination of converter and fuel cell controllers. International Journal of Energy Research 29 (12), 1167–1189.

Sun, J., Kolmanovsky, I.V., 2005. Load governor for fuel cell oxygen starvation protection: a robust nonlinear reference governor approach. IEEE Transactions on Control Systems Technology 13 (6), 911–920.

Tekin, M., Hissel, D., Pera, M.C., Kauffmann, J.M., 2006. Energy consumption reduction of a PEM fuel cell motor-compressor group thanks to efficient control laws. Journal of Power Sources 156 (1), 57–63.

Wang, C., Nehrir, M.H., Gao, H., 2006. Control of PEM fuel cell distributed generation systems. IEEE Transactions on Energy Conversion 21 (2), 586–595.

Wang, C.Y., 2004. Fundamental models for fuel cell engineering. Chemical Reviews 104, 4727–4766.

Weber, A.Z., Newman, J., 2004. Modeling transport in polymer-electrolyte fuel cells. Chemical Reviews 104, 4679–4726.

Wilkinson, D.P., Vanderleeden, O., 2003. In: Vielstich, W., Gasteiger, H., Lamm, A. (Eds.), Handbook of Fuel Cells. Wiley, London, pp. 315–324.

Woo, C.H.K., 2006. A study of stirred tank reactor polymer electrolyte membrane fuel cell stack dynamics. Senior Thesis. Chemical Engineering. Princeton University.

Xue, X., Tang, J., Smirnova, A., England, R., Sammes, N., 2004. System level lumped-parameter dynamic modeling of PEM fuel cell. Journal of Power Sources 133 (2), 188–204.

Yu, X.C., Zhou, B., Sobiesiak, A., 2005. Water and thermal management for Ballard PEM fuel cell stack. Journal of Power Sources 147 (1–2), 184–195.

Zawodzinski, C., Møller-Holst, S, Wilson, M.S., 2000. Efficient fuel cell systems. In: 2000 DOE OTT Fuel Cells Program Review, June 7–8. ⟨http://www.pnl.gov/microcats/ottreview/ottmeeting/15-Wilson.pdf⟩.

Zenith, F., Skogestad, S., 2006. Control of fuel cell power output. Journal of Process Control, in press.